INTERNATIONAL JOURNAL OF INNOVATIVE RESEARCH & DEVELOPMENT

ISSN 2278 – 0211 (Online)

Factors Effecting Pull Out Behavior of Corrugated Steel Fibres in Cementitious Composites

J. D. Rathod
Applied Mechanics Department, Faculty of Tech. & Engg., MSU, Vadodara, India

Abstract:
Pull out behaviour of steel fibres which are not straight and not circular in shape have received little attention compared to the straight steel fibres. Flat corrugated steel fibres are proved to be very effective at interface during pull out, which results into strain hardening and dissipation of significant amount of cold work energy. Such a performance encourages in development of a unique HPFRCC which is well known as Engineered Cementitious Composite (ECC). All such capabilities can be thoroughly explored by performing single fibre pull out test. In the present experimental study, a single fibre pull out test was performed on MTS machine under displacement control with specially designed fixtures to grip any type of fibre. Corrugated flat steel fibres were embedded in cementitious matrices with 6 mm and 12.5 mm lengths. Cement and sand ratios were adopted as 1: 0.5, 1: 1, 1: 1.5 and 1:2 along with replacement of cement by fly ash as 10%, 20% and 30%. Load was recorded at peak and corresponding pull out energy is calculated. De-bonding and pull out behaviour are evaluated qualitatively. Effects of fibre length, cement and sand ratio and fly ash percentage on pull out behaviour of flat corrugated fibre in cementitious composite are discussed in detail. This will help in developing the corrugated steel fibre based ECC.

1. Introduction

ECC is one of the micromechanically optimized high performance fibre reinforced cementitious composites (HPFRCC) without coarse aggregates. The optimization methodology by Micromechanics principle makes ECC different in the family of HPFRCCs. Optimization of the fibre properties is one of the important micromechanical parameters involved in micromechanics that leads to unique ductile performance of this composite [1]. Several researches have been carried out to explore the capabilities of synthetic fibres in the ECC. Synthetic fibres provide suitable properties to satisfy ECC performance criteria of strain hardening with multiple cracking. But a study on steel fibre has received less attention, though it has varieties of cross sections and surface deformations for providing better bond, mechanical anchorage and pull out resistance. Naaman [2] has reported extensive work on engineered steel fibres of various cross sections for reinforcement in cementitious composites. Fibres with non-circular cross sections can be characterized by Fibre Intrinsic Efficiency Ratio (FIER) to represent a better fibre - matrix reinforcing effectiveness. There are four bond components e.g. adhesion, friction, mechanical and interlock. Three of the bond components namely; friction, mechanical and interlock can be optimized by adopting scientific approach for fibre cross section and geometry. When the fibre is made of a deformed hot or cold drawn wire, after debonding, it pulls out in its initial path with minor matrix internal degradations and gets straightened after complex extraction dissipating significant amount of plastic energy [3]. This mechanism can be further enhanced by improving frictional component of bond by providing flat lateral geometry. Although, modulus of elasticity gets reduced due to corrugation, plastic deformation of fibre during pull out facilitates large slip displacement [4, 5]. This has significant implications at the composite level where cracks can be constrained by the fibres up to very large crack widths. Therefore, flat corrugated steel fibres are most attractive out of other different types of fibres available in the market for use in special applications.

The method for directly assessing fibre/matrix interfacial parameters is to pull a single fibre out of its surrounding matrix. Fibre-matrix interfacial properties are important in controlling macroscopic properties of composite materials. Straight steel fibres exhibit slip softening behavior after the debonding in load-slip displacement graph [6]. Corrugated steel fibres exhibit slip hardening behavior after debonding because of its geometry. Straightening of the fibre along with increasing load carrying capacity because of corrugation effect makes it possible to get large slip displacement up to peak load. This mechanism is known to be ductile slip hardening effect [7,8]. Mechanical anchorage and length of the fibre play primary role on the maximum value of the peak load, while matrix plays a secondary role during slipping process of the pull out mechanism. Matrix must be suitably designed so that it allows the fibre to pull out without rupture of the fibre or spalling of the matrix itself. Matrix properties can be controlled by cement: sand ratio and replacement of cement by fly ash. Fly ash is the most attractive pozolanic material and is used all over the world due to so many beneficial effects. ECC has been successfully developed by using Recron fibres which are of polyester type and mechanical properties of which are studied by considering various parameters [9, 10]. Corrugated steel fibres can elevate performance of ECC, provided its micromechanical properties are well studied and incorporated in development of composite. The present work aims at studying the various micromechanical parameters of corrugated steel fibres in cementitious composites for developing more stronger and ductile ECC.

2. Material Composition, Specimen Preparation and Test Set Up

Kamal brand 53 grade OPC, 300 μ passing silica sand, w/c ratio of 0.35, 1% dose of conplast SP 430 brand concrete super plasticizer were used in cementitious matrices. Cement: sand ratios were adopted for matrices as 1:0.5, 1:1, 1:1.5 and 1:2. Xorex type corrugated flat steel fibers of embedded lengths (l_e) 6 mm and 12.5 mm were used to study pull out behavior in cementitious matrices. Pictorial view of steel fiber and briquette type pull out specimen are shown in Figure 1. Steel fibers posses tensile strength 825 MPa and specific gravity of 7.6. Fly ash used for the present investigation is a processed siliceous pulverized ash confirming to IS 3812 (Part 1): 2003. Steel fibres of 30 mm length were supplied by the manufacturer. Required embedded lengths of 6 mm and 12.5 mm were provided in the matrix by using mould of extended briquette specimen. Fibre was kept in aligned position in the center of two ends of briquette mould with the help of two halves of straight portion of wooden mould.

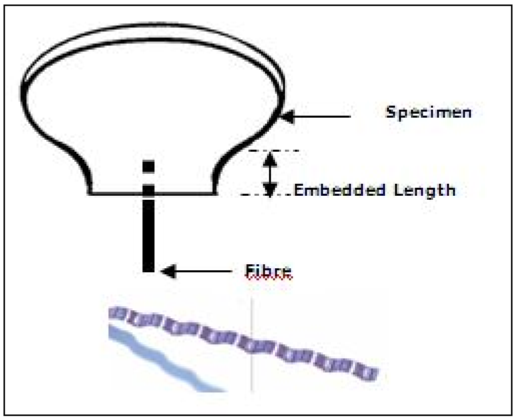

Figure 1: Steel fibre and pull out specimen

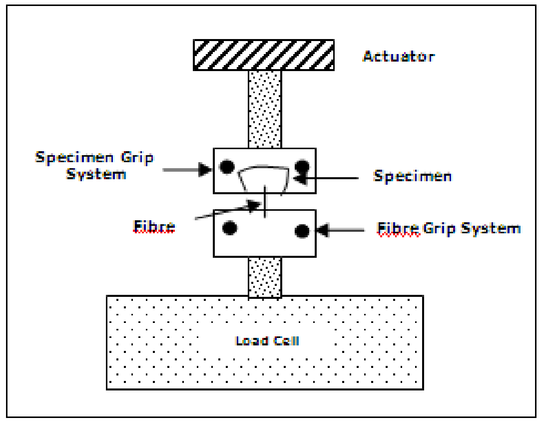

Figure 2: Test set up for fibre pull out

Matrix portion of the specimen was gripped in upper fixture while fibre was gripped in the lower fixture. Due care was taken to keep the minimum possible fibre free length while gripping. Upper fixture was fixed to the actuator of MTS machine while lower fixture was fixed to the load cell as shown in the Figure 2. Pull out load was applied at displacement control rate of 0.005 mm per second. Load-Displacement graphs were obtained on computer by automatic data acquisition system. Movement of actuator of MTS machine served as pull out displacement on XX axis and load sensed by load cell served as pull out load on YY axis of the presented graphs. Total 6 specimens were tested after 28 days of normal water curing for each matrix. Average of best 3 results is considered for the discussion. Load-Pull out curves presented here are of reliable and best one out of 6 specimens for each matrix.

3. Test Results and Discussion

Figure 3 represents pull out behavior of steel fibers in different matrices with 6 mm embedment length whereas Figure 4 depicts the pull out curves for 12.5 mm embedment length. All these curves reflect general behavior observed during the test which can be described as follow. The shape of load-displacement curves is found same for all cases. The fibre pull out in beginning was elastic and perfectly reversible. The fibre and the matrix were bonded over the entire length, because the maximum shear stress at their interface did not exceed. The deformation of fibre and matrix was compatible. This is referred as Bend over Point (BOP) where breakage of elastic fibre-matrix bond occurs. Very steep linear curve is observed up to BOP in load-displacement graphs. The fibre-matrix anchorage allowed the pull out to continue at about the same or a higher load than that of BOP. The shape of curve depends upon matrix strength, geometry of the fibre. Region past BOP but before peak was where fibre developed its full anchorage. After BOP, fibre slowly developed full anchorage and approached ultimate condition up to occurrence of peak pull out load behaving none linearly.

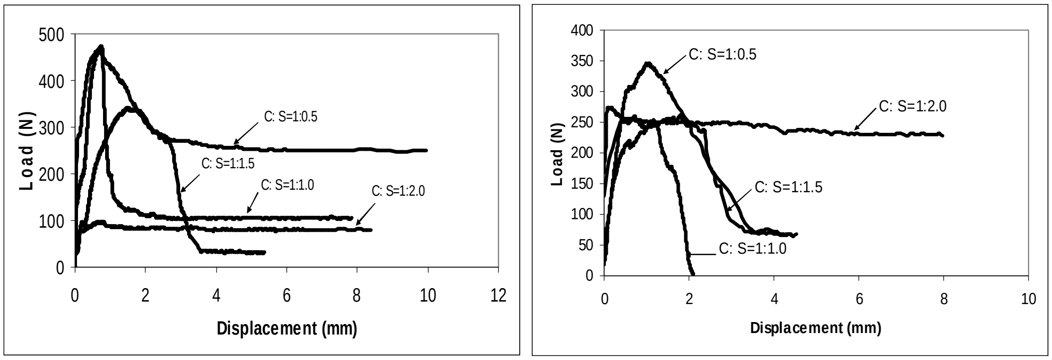

(a) 0% fly ash *(b) 10% fly ash*

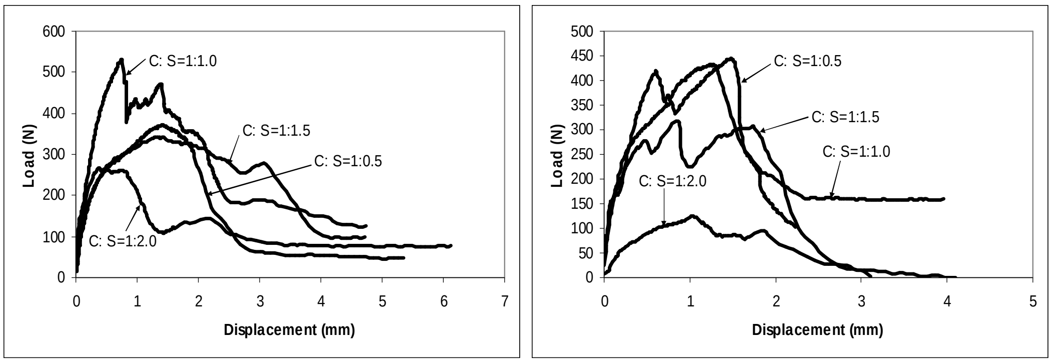

(c) 20% fly ash *(d) 30% fly ash*

Figure 3: Effect of C: S ratio on pull out behavior with different fly ash replacement (6 mm)

The maximum load that can be supported by the fibre reached after the fibre started to slip within its initial print and not at the time where it was totally debonded unlike synthetic fibre. Moreover, during the pull out process, some friction developed along the initial print at the fibre/matrix interface. The matrix played a secondary role during the slipping process compared to the mechanical anchorage. Once fibre started to move, the friction between the fibre and matrix determined the post peak behavior which was more significant in case of a flat lateral geometry as reflected in all curves.

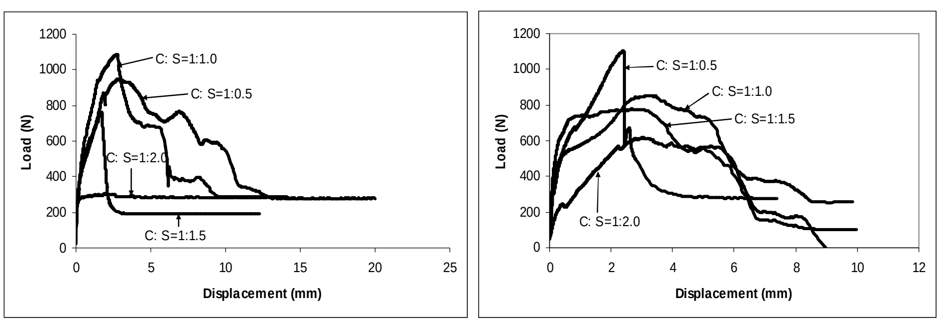

(a) 0% fly ash *(b) 10% fly ash*

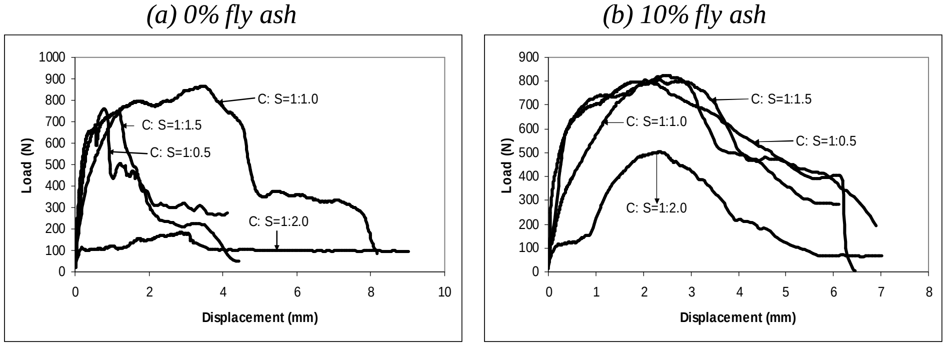

(c) 20% fly ash *(d) 30% fly ash*

Figure 4: Effect of C: S ratio on pull out behavior with different fly ash replacement (12.5mm)

The pull out of the fibre observed was according to following four modes. In the first mode, the fibres kept their initial corrugated shape during the process because the poor matrix was completely destroyed in the fibre area and the embedded length was small i.e. 6 mm long steel fiber embedded in a matrix with C: S ratio of 1: 1.5 and 1: 2.0. Post peak behavior in this mode of failure was oscillatory or a cyclic type that can be characterized as a way that non uniform section moves in its surrounding tunnel of matrix. In second mode, matrix was not damaged at all and was stronger during the slipping process due to which fibre became almost straight. Some polishing action by the fibres during its pull out was observed. This mechanism was observed in the matrix having C: S ratio of 1: 0.5 with 6 mm and 12.5 mm embedded lengths. In third mode, the matrix was partially damaged around the fibre area and completely damaged at the entry of the fibre into the matrix. The fibre could deform partially until large cone developed at the entry and then it pulled out suddenly as in case of matrix with C: S of 1: 1.5 and 1:2.0 with 12.5 mm embedded length. In the fourth mode, steel fibre ruptured at a location where it was gripped due to stress concentration and heavy load. This mechanism was observed for a 12.5 mm embedment length in the stronger matrix i.e. C: S ratio of 1: 0.5 and 1: 1.0. Frequency of fibre breakage reached up to 20% in a cementitious matrix with fly ash replacement of 30%, being brittle in nature. This mode of failure was observed because of fibre gripping arrangement. First three pull out modes were observed simultaneously in matrices with C: S ratio of 1:1, 1:1.5 and 1:2.

3.1. Effect of cement and sand ratio on pull out behavior

Figures 3 and 4 explain effect of C: S ratio on pull out behavior of steel fibres with 6 mm and 12.5 mm embedment lengths and different fly ash replacements. The shape of pull out curve was almost same for all C: S ratios for a given length of fibre and fly ash replacements. They are composed of a first step ascending linear part followed by the non linear curve until a maximum load is recorded. Throughout this process the fibre worked exclusively in traction with plastic deformation and necking. Thus, significant amount of cold work energy was released in this process. Actually, fibres are mainly added in the matrix for energy absorption requirement. Increase in the matrix strength is secondary expectation by fibre addition. Therefore, peak load should not be the only criteria of evaluation of performance of fibre reinforced composite but rather pull out energy would also be the appropriate criteria. Especially for deformed fibres, load at BOP is only the representative parameters for bond, beyond which plastification would result in slip with sustained load. So, peak load and pull out energy are two different aspects and they need not to be of the same trend while keeping other parameters constant.

Tables 1 to 4 indicate load and Tables 5 to 8 indicate pull out energy at different levels for various C: S ratios. To begin with the pull out behavior, load at BOP was first recorded. This load decreased as sand content increased which is clearly reflected in the results. Infect elastic deformation of matrix and fibre and bearing component are also included in the load at BOP. With the bigger core of matrix taking part in the transfer of load, the effects of matrix strength become more important in case of deformed fibre. In previous study [9] it was observed that compressive strength of matrix increases with decrease in sand content. In the same fashion, energy at BOP also decreases with increase in sand content. Slope of linear portion up to BOP remains almost same for all cement: sand ratios. Fibre deformation did not effect on load at BOP. There was a compatible deformation of fibre and matrix with C: S ratio of 1: 0.5 and 1: 1.0 up to high range of load at BOP.

Fly Ash	**BOP Load (N)**		**Debonding Load (N)**		**Peak Load (N)**	
l_e (mm) →	6 mm	12.5 mm	6 mm	12.5 mm	6 mm	12.5 mm
0%	120.14	280.78	234.37	608.12	661.94	927.06
10%	120.70	332.36	253.63	674.99	290.88	902.83
20%	126.50	346.51	294.93	734.41	326.24	801.34
30%	131.17	345.03	351.16	774.41	410.90	833.86

Table 1: Load at different levels for C: S ratio of 1: 0.5

Fly Ash	**BOP Load (N)**		**Debonding Load (N)**		**Peak Load (N)**	
l_e (mm) →	6 mm	12.5 mm	6 mm	12.5 mm	6 mm	12.5 mm
0%	90.97	181.97	152.34	555.60	395.33	880.28
10%	104.66	290.36	185.42	603.16	226.74	749.52
20%	119.91	243.67	229.79	609.97	484.69	752.36
30%	120.31	293.41	265.02	693.65	427.60	804.38

Table 2: Load at different levels for C: S ratio of 1: 1

Fly Ash	**BOP Load (N)**		**Debonding Load (N)**		**Peak Load (N)**	
l_e (mm) →	6 mm	12.5 mm	6 mm	12.5 mm	6 mm	12.5 mm
0%	47.47	154.90	114.45	507.40	260.44	759.40
10%	99.09	206.84	151.31	513.78	274.67	717.52
20%	110.89	208.41	174.26	563.00	277.13	751.41
30%	113.42	236.32	237.93	607.76	268.41	670.65

Table 3: Load at different levels for C: S ratio of 1: 1.5

Fly Ash	BOP Load (N)		Debonding Load (N)		Peak Load (N)	
l_e (mm) →	6 mm	12.5 mm	6 mm	12.5 mm	6 mm	12.5 mm
0%	38.07	71.13	57.80	77.53	83.91	212.29
10%	44.78	99.52	84.57	140.14	142.63	389.82
20%	51.92	96.68	123.33	156.68	158.75	176.98
30%	60.81	102.19	167.27	192.19	198.91	325.51

Table 4: Load at different levels for C: S ratio of 1: 2

Fly Ash	BOP		Debonding		Peak (PE)		Post Peak (PPE)		PPE/PP	
l_e (mm) →	6	12.5	6	12.5	6	12.5	6	12.5	6	12.5
0%	0.011	0.052	0.139	0.182	0.380	1.320	1.399	3.772	3.68	2.85
10%	0.019	0.060	0.142	0.220	0.334	1.260	1.200	3.327	3.59	2.64
20%	0.023	0.062	0.169	0.318	0.362	0.880	1.130	2.550	3.12	2.89
30%	0.033	0.079	0.172	0.439	0.305	0.682	0.524	2.249	1.71	3.29

Table 5: Pull-out energy (N-m) at different levels for C: S ratio of 1: 0.5

Fly Ash	BOP		Debonding		Peak (PE)		Post Peak (PPE)		PPE/PP	
l_e (mm) →	6	12.5	6	12.5	6	12.5	6	12.5	6	12.5
0%	0.005	0.045	0.130	0.163	0.281	1.559	0.658	3.655	2.34	2.34
10%	0.007	0.050	0.142	0.179	0.293	1.228	0.446	3.286	1.52	2.68
20%	0.012	0.058	0.154	0.300	0.279	1.434	0.339	3.123	1.21	2.17
30%	0.018	0.059	0.166	0.339	0.384	1.323	0.289	3.082	0.75	2.33

Table 6: Pull-out energy (N-m) at different levels for C: S ratio of 1: 1

Fly Ash	BOP		Debonding		Peak (PE)		Post Peak (PPE)		PPE/PP	
l_e (mm) →	6	12.5	6	12.5	6	12.5	6	12.5	6	12.5
0%	0.003	0.020	0.066	0.132	0.154	0.821	0.404	2.798	2.62	3.41
10%	0.007	0.032	0.104	0.154	0.338	1.668	0.325	2.235	0.96	1.33
20%	0.012	0.034	0.105	0.260	0.195	1.782	0.324	2.132	1.67	1.20
30%	0.017	0.041	0.117	0.290	0.187	0.721	0.203	2.020	1.08	2.80

Table 7: Pull-out energy (N-m) at different levels for C: S ratio of 1: 1.5

Fly Ash	BOP		Debonding		Peak (PE)		Post Peak (PPE)		PPE/PP	
l_e (mm) →	6	12.5	6	12.5	6	12.5	6	12.5	6	12.5
0%	0.001	0.010	0.008	0.027	0.057	0.293	0.386	1.883	6.77	6.43
10%	0.004	0.014	0.012	0.014	0.038	0.731	0.303	1.755	7.97	2.40
20%	0.007	0.015	0.019	0.145	0.091	0.339	0.297	1.753	3.26	5.17
30%	0.011	0.030	0.022	0.053	0.094	0.465	0.191	1.001	2.03	2.15

Table 8: Pull-out energy (N-m) at different levels for C: S ratio of 1: 2

Post peak energy which is one of the most important parameters, reduces with the increase in sand content. Ratio of post peak energy to peak energy is suggested as a criterion for the FRC performance. Although, this ratio show scattering behavior, but one can judge post peak behavior of the matrix with relation to pre peak behavior to evaluate the composite performance. This ratio is consistent in the matrix with C: S ratio of 1: 0.5 whereas lots of variation is observed for the other matrices. Cementitious matrix with C: S ratio of 1: 0.5 is a high strength matrix. Failure patterns in about 80% specimens of this matrix were of first mode only. Therefore, some uniformity was observed in the matrix with C: S ratio of 1: 0.5. Whereas other matrices were having combined action of matrix degradation due to which results were not consistent.

3.2. Effect of fly ash on pull out behavior

Fly ash replacement was limited to 30% in the matrix. As compressive strength increases with increase in fly ash [10], load at BOP, and debonding increased with increase in fly ash replacement. Pull out energy at BOP and debonding also increase with the fly ash replacement. Contribution of fly ash is significant up to debonding. Adhesional component of bond is much improved by fly ash due to densification effect. Bearing component is also enhanced by fly ash up to debonding. But when fibre started to pull out, degradation by bearing was very fast due to which splitting of matrix and fibre tunnel degradation became more severe. Frictional component of bond is adversely affected by addition of the fly ash due to which degradation in post peak behavior is noticed in pull out curves of matrix having C: S ratio of 1: 0.5 and 1:1. As fly ash introduced brittleness, post peak energy reduces with increase in fly ash replacement. Therefore, the ratio of post peak to peak energy decreases with increase in fly ash replacement for C: S of 1: 0.5 and 1: 1.0.

3.3. Effect of length of fibre on pull out behavior

The shape of pull out versus end slip response does not change with change in embedment length. For deformed fibres, since, the number of surface indentations increase with increase in embedment length, effect is seen in ascending branch with larger resistance. More was the length, more was the peak load, and bigger was the crushed cone size. Consequently more was the unfolding on a greater freed length at peak load which directly influenced the displacement at peak; increases the pull out energy. Slope of peak load increases with increase in length of fibre. In case of 6 mm embedded fibres, the cone crush in poor matrix within very short embedded length governed the failure mechanism due to which fibre unshaping during pull out was not observed. Fibre deformations are effective in enhancing the pull out resistance of fibres only so long as complete fibre pulls out with plastic deformation occurres. Weaker matrix did not provide sufficient anchorage. Therefore, post peak/ peak energy ratio is found to be the maximum in C: S of 1: 0.5 matrix for 6 mm embedded length without fly ash replacement. Whereas, this ratio is the maximum for 12.5 mm length of fibre in the same matrix having C: S ratio of 1:0.5 with 30% fly ash replacement. Failure patterns at exit point in the matrix with C:S ratio of 1:0.5 for 6 mm and 12.5 mm fibre embedded lengths are shown in Figures 5 (a) and (b) respectively.

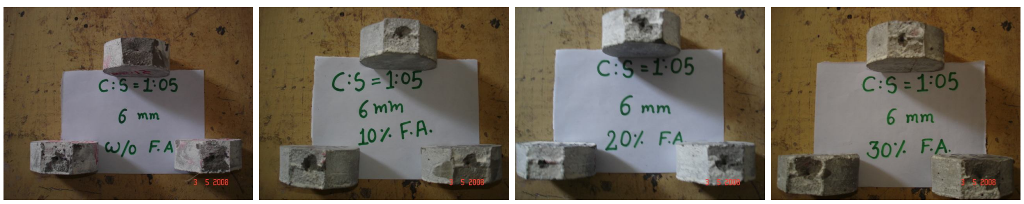

(a) 6 mm fibre embedded samples with fly ash variation

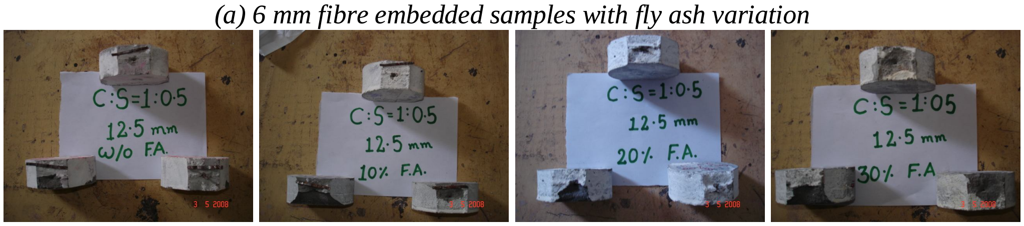

(b) 12.5 mm fibre embedded samples with fly ash variation

Figure 5: Failure patterns at fibre exit point in the matrix with C: S ratio of 1:0.5

Very interesting observation was that in pull out behavior of all the matrices that half the embedded length contributed to pull out resistance of about 90% and then pull out behavior was almost insignificant. Also, it was noticed that $1/4^{th}$ length of corrugated flat fibre was effective on either side of the crack for the composite performance.

4. Conclusion

- First three modes of pull out acted simultaneously and varied with the configuration of matrix and even in the same matrix also. This was mainly due to deformed fibres. Bearing, adhesion, and friction component of bond were working together beyond debonding up to peak load. This mechanism may not be exhibited by straight fibre. In few cases, the fibre gripping resulted into the fracture of fibres in the fourth mode.
- Peak load or slip displacement may not be the true representation of behavior in case of deformed fibre but rather pull out energy can be taken as a measure of composite performance. There is an uncertain pull out behavior at peak load.
- As sand content decreases, compressive strength increases due to which load and energy at BOP and debonding increases.
- Post peak performance of the matrix reduces with increase in fly ash replacement unlike pre peak performance. Friction component of bond disproves as fly ash increases. Longer fibre can be supported by the matrix with fly ash due to larger crushed cone size. Whereas, shorter fibre can be more beneficial for use without replacement of cement by fly ash.
- Satisfactorily consistency was observed in pull out behavior of matrix with C: S ratio of 1: 0.5 as most of the pull out specimens failed by first mode.

5. References

1. Li, V.C., 'From micromechanics to structural engineering-the design of cementitious composites for civil engineering application', JSCE Journal of Structural, Mechanical and Earthquake Engineering, 10 (2) (1993) 37-48.
2. Naaman, E., 'Engineered steel fibres with optimal properties for reinforcement of cement composites', Journal of Advanced Concrete Technology, 1 (3) (2003) 241-252.
3. Shannag, M. J., Brincker, R. and Hansen, W., 'Pull-out behavior of steel fibres from cement–based composites', Cement and Concrete Research, 27 (1997) 925-966.
4. Banthia, N. and Trottier, J., 'Concrete reinforced with deformed steel fibres, part 1: bond-slip mechanisms', ACI Materials Journal (1994) 435-446.
5. Banthia, N. and Trottier, J., 'Concrete reinforced with deformed steel fibres, part 2: toughness characterization, ACI Materials Journal (1995) 146-154.
6. Banthia, N., 'A study of some factors affecting the fibre-matrix bond in steel fibre reinforced concrete', Canadian Journal of Civil Engineering, 17 (1990) 610-620.
7. Guerrero, P. and Naaman, A. E., 'Effect of mortar fineness and adhesive agents on pull-out response of steel fibres', ACI Materials Journal, (2000) 12-20.
8. Chanvillard, G. and Pierre-Claude, A., 'Pull-out behavior of corrugated steel fibres- qualitative and statistical results' Advanced Cement Based Material, 4 (1996) 28-41.
9. Rathod, J. D. and Patodi, S. C., 'Effect of cement-sand ratio on shear strength of ECC in 1D and 2D fibre orientation', Civil Engg. and Construction Review Journal, 21 (5) (2008) 86-96.
10. Rathod, J. D. and Patodi, S. C., 'Effect of fly ash on shear, compression, and impact performance of ECC', 'Innovations in Building Materials, Structural Designs and Construction Practices', Proceedings of an International Conference, Erode, May 2008, 149-157.